Оптический журнал

Оптическое приборостроение

Transmission three-port beam splitter and positioning tolerance of the gratings

© 2017 Bo Wang, Hao Pei, Wenhao Shu, Hongtao Li, Li Chen, Liang Lei, Jinyun Zhou

School of Physics and Optoelectronic Engineering, Guangdong University of Technology, Guangzhou 510006, China

E-mail: wangb_wsx@yeah.net

Submitted 21.10.2016

We describe a sandwiched two-layer grating as a three-port beam splitter, which can achieve high-efficiency diffraction with polarization-independence in the 0-th and the ±1-st orders. Diffractive efficiencies of 32.4/32.9% can be diffracted into the 1-st and the 0-th orders for TE polarization. And 33.1/32.8% can be diffracted for TM polarization. Besides, good splitting ratio uniformity can be exhibited within the broad duty cycle for both TE and TM polarizations. Moreover, the positioning tolerance of the gratings that constitute the sandwich is analyzed.

Keywords: *a sandwiched two-layer grating, a three-port beam splitter, diffraction, polarization-independence, TE and TM polarizations.*

OCIS codes: *050.1380; 230.1360; 050.1950*

Трёхпортовый пропускающий светоделитель и чувствительность коэффициентов светоделения к позиционированию решёток

© 2017 г. Bo Wang, Hao Pei, Wenhao Shu, Hongtao Li, Li Chen, Liang Lei, Jinyun Zhou

Описывается двуслойная сендвичеподобная дифракционная решётка, работающая как трёхпортовый светоделитель, обладающий высокой поляризационно-независимой эффективностью дифракции в нулевом и ±1-м порядках. Для ТЕ-поляризации падающего пучка дифракционная эффективность составляет 32,4 и 32,9% в каждом из первых и в нулевом порядках дифракции, соответственно. Для ТМ-поляризации эти величины составляют 33,1 и 32,8%. Как для ТЕ, так и для ТМ-поляризаций равномерность распределения коэффициента светоделения по каналам сохранялась при изменении отношения толщины штриха к шагу решётки в широких пределах. Проанализирована чувствительность коэффициентов светоделения к взаимному расположению составляющих «сендвич» решёток.

INTRODUCTION

The beam splitter is an important element in optical communication, optical computing, and metrology systems, which can separate an incident wave into several beams with good splitting ratio uniformity [1–3]. Gratings have an advantage of compact size [4], whose periods can be comparable to the incident wavelength, only part of diffraction orders can be remained based on the grating equation. Most importantly, the development of micro-fabrication technology makes it possible to produce the beam splitter grating with low cost, low insertion loss, and good performance [5–9]. There are some typical research works related to the three-port beam splitter grating. A diffractive three-port beam splitter has been firstly reported based on a deep-etched grating, which is designed by using rigorous coupled-wave analysis (RCWA), where the experimental results are in good agreement with the theoretical values [10]. A high-efficiency three-port beam splitter of reflection grating with a metal layer has been reported, which is designed at the duty cycle of 0.5 [11]. K. Patorski et al. presented a three-beam diffraction grating interferometry without self-imaging regime contrast modulations [12]. It can be

seen that most reported beam splitter grating are designed for the special prescribed duty cycle. It is very desirable that a three-port beam splitter grating can have the merit of wide duty cycle range.

In this letter, a high-efficiency three-port beam splitter based on a sandwiched two-layer grating is proposed for transmission. The profile parameters optimized are given by numerical calculation using RCWA to achieve three-port output with high efficiency and uniformity [13]. Such a beam splitter can have the polarization-independent property, which can separate the incident wave into the ±1-st and 0-th transmission orders with good splitting ratio uniformity for both TE and TM polarizations. Compared with the reported three-port beam splitters, the performance can be improved greatly, including the efficiency, the aspect ratio of the grating depth to the ridge width, especially the duty cycle range. The novel structure presents a helpful access of grating element in practice effectively.

DESIGN AND OPTIMIZATION

The sandwiched two-layer sandwiched grating is show in fig. 1. The novel structure is composed of the fused-silica substrate, the Ti_2O_5 layer with the depth of h_1 and the refractive index $n_1 = 2$, the fused-silica layer with the depth of h_2 and the refractive index $n_2 = 1.45$, and the covering layer of fused silica. Compared with existing surface-relief grating, it is easy to clean and protect the grating surface based on a sandwiched structure. An unpolarized plane wave with the wavelength of $\lambda = 800$ nm is incident upon the grating with the duty cycle of f and the period d under normal incidence. As a three-port beam splitter, the grating can be designed to separate energies into the 0-th and the ±1-st diffracted orders based on the vector diffraction theory.

In this design, a usual duty cycle of 0.5 is chosen, which is easy for fabrication. The next step is to optimize grating depth of Ti_2O_5 and grating depth of fused silica to achieve high transmission efficiencies for both TE polarization and TM polarization. The RCWA can give a stable and efficient implementation of the transmission sandwiched grating by the numerical calculation. Firstly, the sandwiched grating is divided into a large number of thin slabs. The electromagnetic fields can be expressed as the space-harmonic expansion in each slab. By numerical calculation, the exact result is given. And the electromagnetic boundary conditions are applied at interfaces from the top to the bottom for all the thin slabs. The next, diffracted amplitudes and efficiencies can be yielded. The grating can be potentially used as a diffractive three-port beam splitter. Different Maxwell's equations for electromagnetic fields are applied in RCWA for TE and TM polarizations. During calculation, the detection way is to calculate efficiency ratio between the 1-st and the 0-th order, where the ratio of around 1 means the three-port beam splitter with good performance.

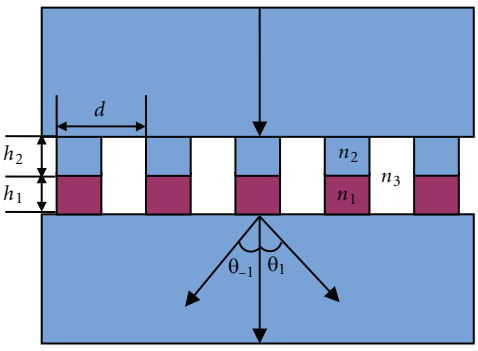

Fig. 1. Schematic configuration of a transmission three-port beam splitter based on sandwiched double-layer grating.

The contour of the efficiency's ratio between the 1-st and the 0-th diffractive orders of the grating versus grating depth of h_1 and depth of h_2 is depicted for TE-polarized and TM-polarized waves, respectively, as shown in fig. 2. The value of efficiency's ratio can reach 0.984 for TE polarization and efficiency's ratio is 1.008 for TM polarization at the grating period of 930 nm. The three-port beam splitter grating can separate TE polarization with efficiency of 32.4% in the 1-st reflected order and 32.9% in the 0-th

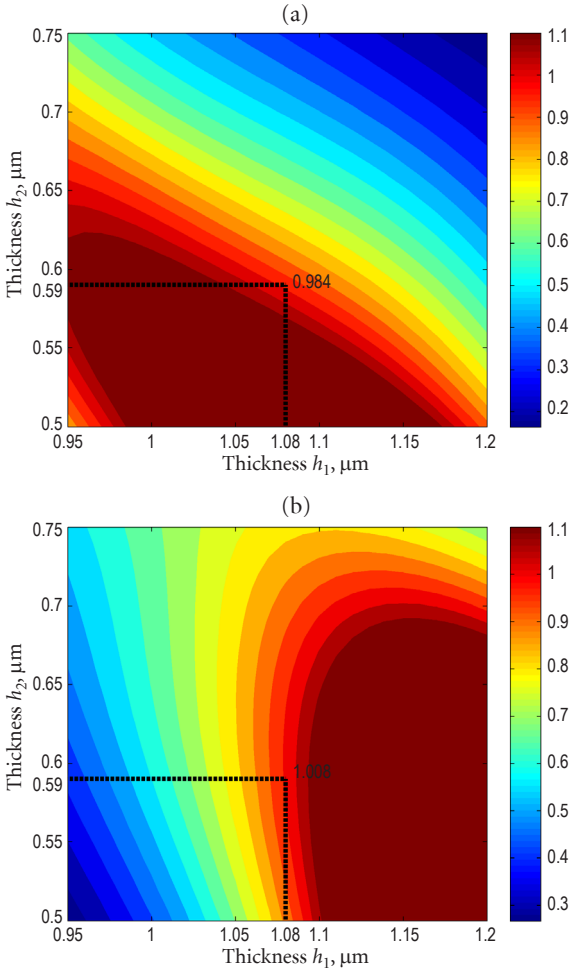

Fig. 2. Contour of efficiency's ratio between the 1-st and 0-th orders of the grating versus grating groove depths of first and second layers with the duty cycle of 0.5 and the incident wavelength of 800 nm under normal incidence: (a) TE polarization; (b) TM polarization.

reflected order. For TM polarization, 33.1% and 32.8% can be separated into the two orders with depth of $h_1 = 1.08$ μm and $h_2 = 0.59$ μm.

PERFORMANCE AND INCIDENT BANDWIDTH

The diffractive three-port beam splitter has been presented based on a sandwiched grating in this paper, which is operated at the grating period of 930 nm, the duty cycle of 0.5. It is necessary to improve the bandwidth not only for the grating period but also for the duty cycle for practical fabrications. Figure 3 shows diffraction efficiency of the sandwiched transmission three-port beam splitter grating versus grating period with the duty cycle of 0.5 and incident wavelength of 800 nm. In fig. 3, efficiencies of three orders are both more than 32% for TE polarization within the range of 927–933 nm. Moreover, the grating can diffract efficiencies more than 32% for TM polarization within the wide bandwidth of 915–936 nm.

Figure 4 shows the diffraction efficiency of a sandwiched transmission three-port beam splitter grating versus incident wavelength under normal incidence with the $h_1 = 1.08$ μm and $h_2 = 0.59$ μm, where the aspect ratio of the grating depth to the ridge width is 2.32 for the first layer and 1.26 for the second layer, which can be etched in fused silica easily and effectively. Besides, efficiencies of three orders are more than 32% for both TE and TM polarization within the incidence wavelength of 798–806 nm. Figure 5 shows the diffractive efficiency of a sandwiched transmission three-port beam splitter grating versus duty cycle under normal incidence for the grating period of 930 nm with depth of 1.08 μm for the first layer and depth of 0.59 μm for the second layer. One can see that efficiencies of three orders more than 32% for both TE polarization and TM polarization can be achieved within the duty cycle range of 0.491–0.52.

After the superimposing of gratings, it may occur that the resulting sandwich would look like fig. 6, where Δ_1 is the error of the alignment of the edges of the grooves, and Δ_2 is the residual gap between grooves. If these $\Delta_{1,2}$ are not equal to zero, the condition of the efficiency more than 32% can be violated. So, such misalignments violate the proximity to unity of the ratio of intensities of the separated beams. However, within the range of $\Delta_1 < 2$ nm and $\Delta_2 = 0$ or the range of $\Delta_1 = 0$ nm and $\Delta_2 < 5$ nm, the condition of the efficiency more than 32% would still be realized.

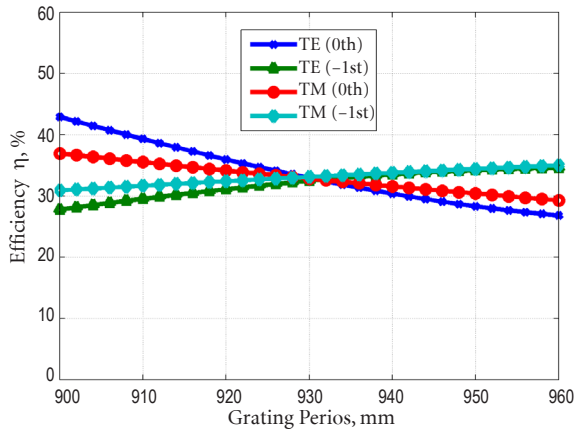

Fig. 3. Diffraction efficiency of a sandwiched transmission three-port beam splitter grating versus grating period under normal incidence with the duty cycle of 0.5 and incident wavelength of 800 nm.

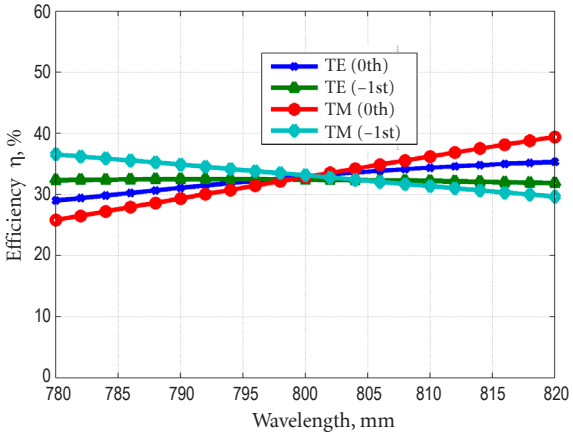

Fig. 4. Diffraction efficiency of a sandwiched transmission three-port beam splitter grating versus incident wavelength under normal incidence with $h_1 = 1.08$ μm and $h_2 = 0.59$ μm.

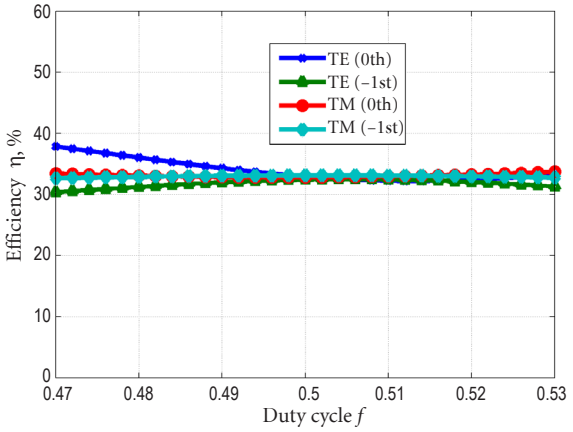

Fig. 5. Diffraction efficiency of a sandwiched transmission three-port beam splitter grating versus duty cycle under normal incidence for the grating period of 930 nm with depth of 1.08 μm for the first layer and depth of 0.59 μm for the second layer.

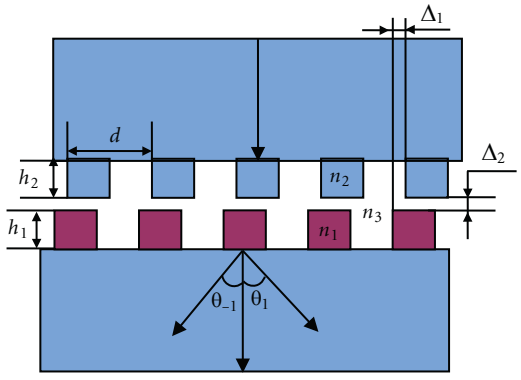

Fig. 6. Schematic structure for misalignments after the superimposing of gratings.

CONCLUSIONS

In conclusion, a mixed metal sandwiched two-layer grating is presented for diffractive three-port beam splitter with high-efficiency and wide duty cycle bandwidth. RCWA can be applied to optimize the microstructure grating parameters. Diffraction efficiencies of 32.4% and 32.9% can be obtained in the ±1-st and the 0-th orders for TE polarization and 33.1% and 32.8% for TM polarization can be achieved with grating period of 930 nm, duty cycle of 0.5, $h_1 = 1.08$ μm and $h_2 = 0.59$ μm under normal incidence. For different grating period and duty cycle, efficiencies of more than 32% for TE polarization and TM polarization in the 1-st and 0-th orders can be obtained within the period range of 927–933 nm and duty cycle range of 0.491–0.520, while the aspect ratio of the first depth/second depth to the ridge width is 2.32/1.26, which can be etched in fused silica easily and effectively. It would be very useful for practical applications.

This work is supported by the National Natural Science Foundation of China (11304044), the Excellent Young Teachers Program of Higher Education of Guangdong Province, and the Pearl River Nova Program of Guangzhou (201506010008).

REFERENCES

1. *Lysenko G.A., Kachurin Yu.Yu., Pogodaev V.V., Shamilina E.V.* Dependence of the error of measurement of the phase delay by an interference ellipsometer on the polarization properties of the beam splitter // J. Opt. Technol. 2002. V. 69. P. 505.
2. *Pan C., Rahman B.M.A.* Compact polarization-independent MMI-based 1Ч2 power splitter using metal-cap silicon-on-insulator waveguide // IEEE Photon. J. 2016. V. 8. P. 7101014.
3. *Jiao W., Wang G., Ying Z., Kang Z., Sun T., Zou N., Ho H.-P., Zhang X.* Optofluidic switching of nanoparticles based on a WDM tree splitter // IEEE Photon. J. 2016. V. 8. P. 7803010.
4. *Wu D., Xie H., Dai X., Wang R.* A novel method to fabricate micro-gratings applied for deformation measurement around a crack in a thin film // Meas. Sci. Technol. 2014. V. 25. P. 025012.
5. *Ye T., Fu Y., Qiao L., Chu T.* Low-crosstalk Si arrayed waveguide grating with parabolic tapers // Opt. Express. 2014. V. 22. P. 31899.
6. *Zheng G., Chen Y., Xu L., Su W., Liu Y.* High reflectivity broadband infrared mirrors with all dielectric subwavelength gratings // Opt. Commun. 2014. V. 318. P. 57.
7. *Wang B., Chen L., Lei L., Zhou J.* Metal-based phase grating for high-efficiency polarizing beam splitter // Opt. Commun. 2013. V. 296. P. 149.
8. *Zhao H., Yuan D.* Design of fused-silica rectangular transmission gratings for polarizating beam splitter based on modal method // Appl. Opt. 2010. V. 49. P. 759.
9. *Dai M., Wan W., Zhu X., Song B., Liu X., Lu M., Cui B., Chen Y.* Broadband and wide angle infrared wire-grid polarizer // Opt. Experss. 2015. V. 23. P. 15390.
10. *Feng J., Zhou C., Wang B., Zheng J.* Three-port beam splitter of a binary fused-silica grating // Appl. Opt. 2008. V. 47. P. 6638.
11. *Shu W., Wang B., Li H., Lei L., Chen L., Zhou J.* High-efficiency three-port beam splitter of reflection grating with a metal layer // Superlattice. Microst. 2015. V. 85. P. 248.
12. *Patorski K., Trusiak M., Pokorski K.* Diffraction grating three-beam interferometry without self-imaging regime contrast modulations // Opt. Lett. 2015. V. 40. P. 1089.
13. *Moharam M.G., Pommet D.A., Grann E.B.* Stable implementation of the rigorous couple-wave analysis for surface-relief grating: enhanced transmittance matrix approach // J. Opt. Soc. Am. A. 1995. V. 12. P. 1077.